Raman Investigation of the CO_2 Complex Formation in CO_2−Acetone Mixtures

M. Besnard,*,† M. Isabel Cabaço,‡ S. Longelin,† T. Tassaing,† and Y. Danten†

Institut des Sciences Moléculaires, CNRS (UMR 5255), Université Bordeaux 1, 351 Cours de la Libération, 33405 Talence Cedex, France, Centro de Física Atómica da UL, Av. Prof. Gama Pinto 2, 1694-003 Lisboa Codex, Portugal, and Departamento de Física, Instituto Superior Técnico, UTL, Av. Rovisco Pais, 1049-001 Lisboa, Portugal

Received: July 19, 2007; In Final Form: September 22, 2007

Polarized and depolarized Raman spectra of CO_2−acetone mixtures have been measured along the isotherm 313 K as a function of CO_2 concentration (0.1−0.9 molar fractions in CO_2) by varying the pressure from 0.2 up to 8 MPa. Upon CO_2 addition, a new band appears at about 655 cm^{-1} and is assigned to the lower frequency $\nu_2^{(1)}$ component of the bending mode after degeneracy removal due to the formation of a 1:1 electron donor acceptor (EDA) CO_2 complex. The equilibrium constant associated with the complex formation was estimated and found close to those of contact charge transfer complexes. The main modifications of the Fermi dyad of CO_2 in the mixtures compared with that of pure CO_2 at equivalent density have been assessed. The band-shape analysis revealed that each dyad component is described by two Lorentzian profiles, showing that a tagged CO_2 molecule probes two kinds of environment in its first shell of neighbors. The first one involves nonspecific interactions of CO_2 with surrounding acetone whereas the second is assigned to the signature of 'transient' CO_2 complexes formed with acetone. An upper bound life time of the complex has been estimated to be 8 ps. In addition, a broad band has been detected between the Fermi dyad peaks at about 1320 cm^{-1} and its origin interpreted as a further evidence of the CO_2−acetone heterodimer formation. Finally, the values of the equilibrium concentration of the heterodimer versus the total concentration of CO_2 deduced from the analysis of the $\nu_2^{(1)}$ band and from the Fermi dyad have been compared, and the difference is interpreted as due to a lack of theoretical approach of Fermi resonance transitions associated with species existing in different environments.

1. Introduction

In a series of papers dealing with the study of supercritical carbon dioxide by Raman scattering,[1,2] we have succeeded to put in evidence the existence of CO_2 homodimers in a reduced density range $\rho^* = \rho/\rho_C$ (where ρ_c is the critical density) extending from 0.2 up to 2 along near critical isotherms $T^* = T/T_C \leq 1.06$ (where T_C is the critical temperature). This conclusion was supported from spectroscopic signatures observed in three spectral domains, namely, the ν_2 bending mode, the $\nu_1-2\nu_2$ Fermi resonance dyad, and the domain extending between the former doublets. Direct evidence of dimeric formation came from the first and third spectral domain in which faint features could be directly assessed to the existence of this state of aggregation. In contrast, the analysis of the Fermi dyad was more indirect, and it was established that the band shape of each component of the doublet resulted from the overlap of two peaks. These peaks could be assigned to particular environments of CO_2. One of the environments was related to molecules interacting to form a homodimer, whereas the second one was associated with carbon dioxide molecules interacting through nonspecific forces (the so-called 'free' molecules). Difficulty was encountered in the analysis of the Fermi dyad band shape as a function of the density. Indeed, near the critical temperature, supercritical fluids (SC) present a rather extended density domain in which local density enhancement (LDE) effects are present and contribute to the observed band centers and widths of the profiles. The aim of the present paper is to continue on this route and to investigate the formation of the heterodimer of CO_2 with a solvent. Acetone has been selected as the solvent for the following reasons. First, it has been established from our ab initio studies that CO_2 interacts with acetone leading to the formation of a 1:1 electron donor−acceptor EDA complex.[3] In this interaction, the carbon atom of CO_2 is the electron acceptor center, and the oxygen atom of the carbonyl group of acetone is the electron donor center. The stabilization energy of the CO_2−acetone heterodimer is greater by at least a factor of two than that of the CO_2 homodimer. As spectral signatures are thought to depend upon the interaction strength between moieties, dimeric formation should be easier to be put in evidence in the CO_2−acetone system. In this context, it is noteworthy to remind that the observation of the splitting of the degenerated ν_2 bending vibration of CO_2 has been considered as a specific spectral signature of the complex.[4,5] Indeed, for an isolated CO_2 molecule, the degenerate ν_2 bending mode frequency is predicted to be at 655.5 cm^{-1}. Due to the EDA interaction, the degeneracy of this mode is removed, and two modes $\nu_2^{(1)}$ and $\nu_2^{(2)}$ assigned, respectively, to the OCO bending motion *in* and *out* of the plane formed by CO_2 and acetone are predicted at 639.6 cm^{-1} and 657.5 cm^{-1}, respectively (cf. Table 1). Recently, we have provided experimental evidence of the existence of such EDA complexes in CO_2–acetone and CO_2–ethanol solutions from Raman spectroscopic measurements in the spectral range of the ν_2 bending mode of CO_2.[6]

* Corresponding author. Tel.: +33 5 40006357. Fax: +33 5 4000 8402. E-mail: m.besnard@ism.u-bordeaux1.fr.

† Université Bordeaux 1.

‡ Centro de Física Atómica da UL and Instituto Superior Técnico.

10.1021/jp0756653 CCC: $37.00
Published on Web 11/30/2007

TABLE 1: Frequency Values $\bar{\nu}$, Raman Scattering Activities I_{Ram}, and Depolarization Ratio ρ Calculated from the MP2 Perturbation Theory Using aug-cc-pVDZ Dunning's Basis Set

vib. mode	CO_2 monomer ν_2(OCO) (cm^{-1})	CO_2−EDA complex (cm^{-1})	I_{Ram} (Å^4)	ρ	ρ_{exp}[a]	$\bar{\nu}_{exp}$[a] (cm^{-1})
ν_2	655.5 (667 IR)[b]					
CO_2−acetone						
$\nu_2^{(1)}$		639.6 (650.8)[c]	12.51	0.47	0.54 ± 0.05	656−659
$\nu_2^{(2)}$		657.7 (669.2)[c]	0.12	0.75		

[a] Experimental frequency $\bar{\nu}_{exp}$ and depolarization ratio ρ_{exp} of the vibrational mode of the band are assigned to the complex formed in CO_2–acetone and CO_2−ethanol mixtures. [b] Reference 11. [c] The ab initio frequency values in parentheses have been corrected (see text).

A last point which must be emphasized is based upon the experimental approach used in our current investigation. It has been shown from thermodynamic studies that upon injecting SC CO_2 under pressure in liquid acetone, two phases exist. In the homogeneous fluid phase, the CO_2 molar fraction can vary from 0.1 up to 0.9 by increasing the pressure from 1 to 8 MPa.[7] Doing that, carbon dioxide passes from the state of solute to the state of solvent. Interestingly, the density of the binary mixtures remains close to that of liquid acetone and increases only by about 10%. Under these conditions, which corresponds to liquid-like density, the LDE phenomenon is irrelevant and any effects observed on the Fermi dyad band-shape can be assessed to the CO_2 state of aggregation. Clearly, the study of the CO_2−acetone mixture presents advantages over the CO_2 neat fluid and will allow shedding light on the heterodimer formation and on the existence of 'free' CO_2 environment without experiencing the difficulties encountered in the analysis of neat CO_2.

In the course of this study, one of the issues that we would also like to address concerns the concept of complex as proposed in the ab initio approach. More specifically, we would like to assess the validity of the interpretation of liquid-state spectra on the grounds of ab initio calculations which only consider a pair of interacting molecules without taking into account the thermal bath (temperature and density) involved in experiments. It could be argued that such a comparison only makes sense for isolated species in a matrix at very low temperature (a few Kelvin). However, molecular dynamics (MD) simulations on the CO_2–H_2O system, also based upon ab initio calculated intermolecular potential, showed that EDA interaction is reflected through the signature of very weak and labile complexes, especially in the calculated radial distribution function $g_{C-O}(r)$ and in the specific hindrance of the rotational dynamics of water.[8−10]

2. Experimental Conditions

The Raman spectra were measured on a Jobin-Yvon HR8000 spectrometer with a Spectra Physics krypton-ion laser source operating at a wavelength of 752.5 nm with a power of 150 mW. The polarized I_{VV} and depolarized I_{HV} spectra were recorded using the back-scattering geometry in two spectral ranges: the former, from 315 to 1140 cm^{-1} with a resolution of 1.8 cm^{-1} using a 600 lines mm^{-1} grating; and the latter, from 1200 to 1450 cm^{-1} with a resolution of 0.5 cm^{-1} using a 1800 lines mm^{-1} grating. To improve the signal-to-noise ratio, several spectra have been accumulated for typical times of 16 min and 4 min, respectively, in the referred spectral ranges. In order to take accurate line positions, the spectrometers have been calibrated by recording different emission lines of a neon bulb. We have used the pressure bench and the Raman cell equipped with fused silica windows previously described[11] to work in the 0.1 to 10 MPa pressure range at $T = 313$ K. For the measurements in the mixtures, we filled the cell more than 80% in volume with acetone (Aldrich, 99.5% purity) in order to ensure that after addition of CO_2 (Air Liquide, purity 99.995%) and pressurization the incident laser beam always impinges on the liquid phase. The mixtures were continuously stirred using a magnet activated by a rotating magnetic field. All the spectra have been recorded after an equilibration time greater than 2 h.

TABLE 2: Values of the Concentration and of the Density in the Liquid Phase of CO_2−Acetone Mixtures as a Function of the Pressure at 313 K[a]

P (MPa)	x_{CO_2} (m.f.)	d (kg m^{-3})	[CO_2] (mol L^{-1})	[acetone] (mol L^{-1})
0.10	0.000	767	0.00	13.2
1.10	0.173	782	2.44	11.6
1.27	0.198	785	2.81	11.4
2.00	0.300	794	4.45	10.3
3.00	0.434	805	6.72	8.77
3.40	0.495	810	7.85	8.00
4.04	0.566	816	9.21	7.07
4.77	0.651	823	11.0	5.87
4.88	0.664	824	11.2	5.69
5.77	0.760	829	13.3	4.20
6.47	0.830	830	14.8	3.04
6.67	0.849	829	15.3	2.71
6.97	0.877	829	15.9	2.23
7.37	0.912	829	16.7	1.61

[a] Values interpolated from ref 7.

The density and pressure−composition of the liquid phase of CO_2 in acetone have been interpolated from published values[7] and are reported in Table 2.

3. ν_2 Bending Mode Spectral Domain

3.1. Experimental Results. The polarized I_{VV} Raman spectrum of neat liquid acetone, measured under its vapor pressure at 313 K, is displayed in the spectral range 625−680 cm^{-1} in Figure 1. Upon addition of CO_2, a new band is detected in the Raman spectrum at a pressure higher than 1.5 MPa as seen from the comparison with that of pure acetone (Figure 1). The band shapes of the polarized and depolarized profiles are well described by Lorentzian functions confirming that a single band is observed (Figure 1). The values of the band center positions of the I_{VV} and I_{HV} profiles are found to be equal and increase linearly with the CO_2 concentration (Figure 2a). The full-widths at half-height (FWHH) of these profiles which are almost identical also increase linearly with the CO_2 content (Figure 2b). The associated depolarization ratio $\rho = I_{HV}/I_{VV}$ is not concentration dependent and has a value of 0.57 ± 0.05 (Figure 2c).

3.2. Interpretation. The interpretation of the observed ν_2 Raman transition of CO_2 in the binary mixture can be performed in the framework of the formation of a 1:1 CO_2−solvent complex as proposed in the ab initio investigation.[3,5,12,13]

Experimentally, the frequency position of the new band is found to be in good agreement with the calculated $\nu_2^{(1)}$ frequency value after correction. This correction consists in

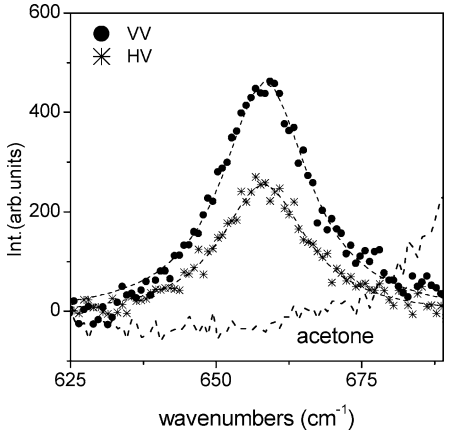

Figure 1. Polarized and depolarized Raman spectra in the spectral domain of the $\nu 2$ bending vibrational mode of CO_2 at 313 K in the CO_2−acetone mixture ($x_{CO_2} = 0.912$): (-•-•-) I_{VV}; (-*-*-) I_{HV}. The background corresponds to the polarized spectrum of pure acetone under vapor pressure. Fitted Lorentzian profiles (---) to ν_2 mode in the mixture are also reported.

multiplying the ab initio $\nu_2^{(1)}$ value by the ratio $\nu_2^{\text{experimental IR}}/\nu_2^{\text{ab initio}} = 667/655.5$. Moreover, a fair agreement is also observed between the measured and the predicted depolarization ratio (Table 1). Therefore, we may infer that the new band observed in the binary mixtures corresponds to the predicted spectral signature for a 1:1 complex formation.

Within this framework, we can write the following reactive scheme

$$\underset{\text{'free'}}{CO_2} + \text{acetone} \rightleftarrows \underset{\text{'bound'}}{CO_2\text{*acetone}} \qquad (1)$$

in which CO_2 can exist either in the so-called 'free' or 'bound' (complex) forms. The new band observed here can be assigned to the CO_2 engaged in this complex, as the CO_2 'free' band is Raman inactive. The equilibrium constant K_C associated with the reactive scheme 1 is given by $K_C = [C_{\text{complex}}]/\{[C_{CO_2}]-[C_{\text{acetone}}]\}$. This constant can be calculated by assuming that the complex concentration $[C_{\text{complex}}]$ is negligible compared with the equilibrium concentrations of $[C_{CO_2}]$ and $[C_{\text{acetone}}]$ and that the latter quantities can be in turn taken from thermodynamical data.[7] To calculate the complex concentration, we have under these hypotheses scaled the integrated intensity of the band of the complex to that of the acetone bands measured for the mixture in the same spectral domain, namely, $r_{//CH_3}$ (1070 cm^{-1}, A_1 symmetry, polarized), δ_{CCC} (376 cm^{-1}, A_1 symmetry, depolarized), δ_{CO} (528 cm^{-1}, B_1 symmetry, depolarized), and γ_{CO} (491 cm^{-1}, B_2 symmetry, depolarized). The integrated intensity I of a solute Raman transition in a mixture is given by:

$$I = CAB\alpha^2 \qquad (2)$$

where C is the molar concentration of the solute, A is a factor depending upon the experimental setup, and α is the matrix element of the derivative of the polarizability tensor versus the normal coordinate of the spectral transition of the isolated solute molecule. The B factor takes into account the variation of the internal field probed by the CO_2 molecule on going from the

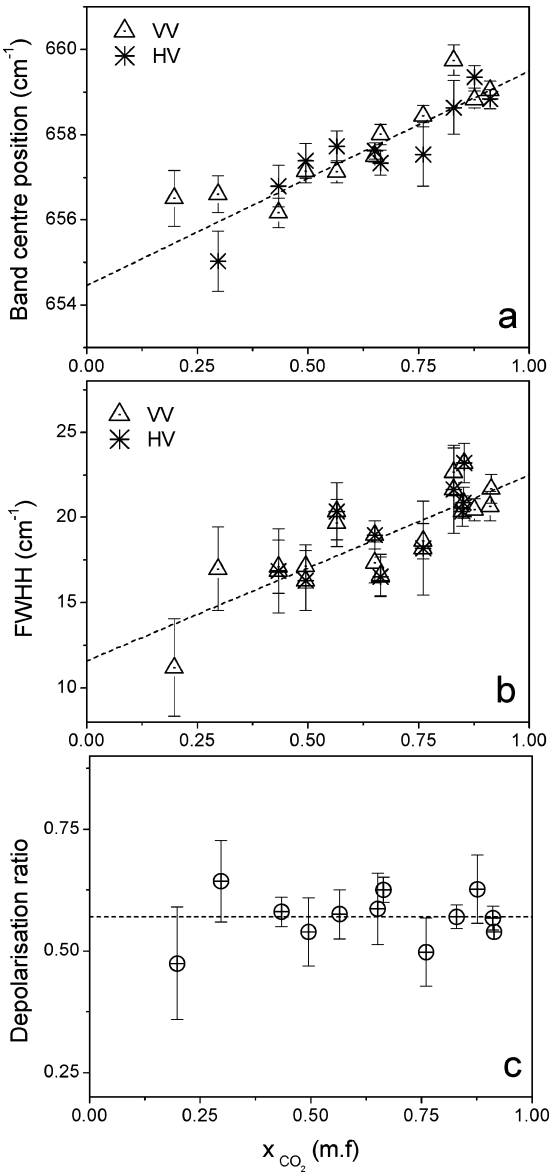

Figure 2. Evolution of the complex band with CO_2 concentration in the CO_2−acetone mixtures: band center position (a) and FWHH (b) of the polarized (Δ) I_{VV} and depolarized (*) I_{HV} profiles; depolarizarion ratio (c).

state of solute in the polar acetone environment to the state of solvent diluting acetone.

Using eq 2, the complex concentration can be calculated as

$$[C_{\text{complex}}] = [C_{\text{acetone}}] \frac{I_{\text{complex}}/\alpha^2_{\text{complex}}}{I_{\text{band}_j\text{ acetone}}/\alpha^2_{\text{band}_j\text{ acetone}}} \qquad (3)$$

taking $[C_{\text{acetone}}]$ from thermodynamical data and using the relative intensity of the spectral transition associated with the complex to that of a particular transition of acetone. However, this treatment requires the knowledge of the $\alpha^2_{\text{band}_j\text{ acetone}}$ value which is associated with a particular acetone transition. The $\alpha^2_{\text{band}_j\text{ acetone}}$ can be calculated from ab initio calculations for the isolated molecule. The difficulty stems from the fact that, in liquid acetone, molecules are somehow aggregated through strong dipolar interactions which may affect as well the corresponding $\alpha^2_{\text{band}_j\text{ acetone}}$. To assess the validity of using the ab initio $\alpha^2_{\text{band}_j\text{ acetone}}$ values in eq 3, we have therefore proceeded as follows. We have first calculated the ratio $I_{\text{band}_i}/I_{\text{ref band}} =$

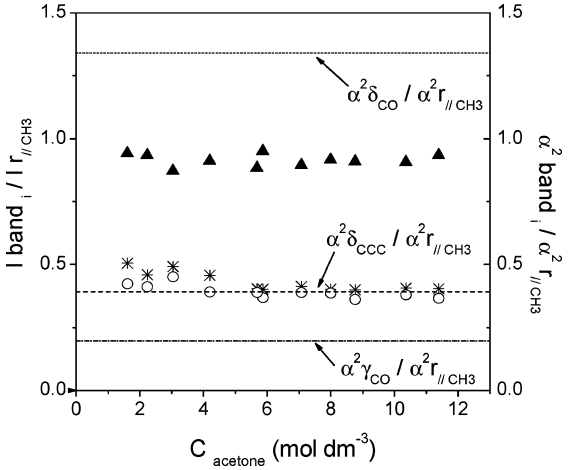

Figure 3. Evolution with acetone concentration of the ratio of the integrated intensities of a band of acetone (band$_i$) and of $r_{//CH_3}$ (taken as a reference band) of acetone in the CO_2−acetone mixture. Band$_i$: (*) δ_{CCC}; (○) γ_{CO}; (▲) δ_{CO}. Values of the ratio of the corresponding ab initio α^2 values calculated for the monomeric acetone molecule are presented for comparison: (- - -) $\alpha^2\delta_{CCC}/\alpha^2 r_{//CH_3}$; (---) $\alpha^2\delta_{CO}/\alpha^2 r_{//CH_3}$; (−·−·−) $\alpha^2\gamma_{CO}/\alpha^2 r_{//CH_3}$. Only for δ_{CCC} are good agreementis obtained.

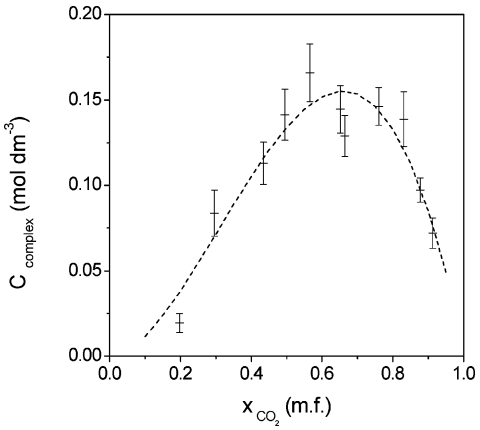

Figure 4. Evolution of the complex concentration with the CO_2 concentration in CO_2–acetone mixture at 313 K (the dash line is only a to guide the eyes).

$\alpha^2_{band_i}/\alpha^2_{ref\ band}$ (see eq 2) of the intensity I_{band_i} of a particular band of acetone in the mixture by the intensity $I_{ref\ band}$ of a band of acetone taken as a reference measured in the same spectral range. The evolution with the concentration of the intensity of the δ_{CCC}, δ_{CO}, and γ_{CO} bands versus the intensity of the $r_{//CH_3}$ band, taken as the reference band, is displayed in Figure 3. The ratios of the corresponding α^2 calculated from ab initio values for the isolated acetone molecules (which are of course independent of the acetone concentration) are also displayed for comparison in the same figure. Clearly, it is only for δ-(CCC) that a good agreement is obtained between the experimental intensity ratio and the calculated α^2 ratio. This result shows that the δ(CO) and γ(CO) vibrations are affected by the state of aggregation of acetone and that their polarizability are different from the calculated value for the isolated molecule.

The complex concentration calculated in eq 3 using the ab initio values of $\alpha^2_{complex}$ and $\alpha^2_{band_i\ acetone}$ of either the δ(CCC) or the $r_{//CH_3}$ vibrations agree within experimental uncertainties. The evolution of the complex concentration with the CO_2 concentration in the mixture is asymmetric with a maximum at $x_{CO_2} \sim 0.65$ (Figure 4). The value of the concentration at the maximum is very low and is only about 1% of the concentration of CO_2 in the binary mixture. From this evolution the equilibrium constant can be estimated for the 1:1 complex with a value for K_C of ~0.0025 l mol^{-1}.

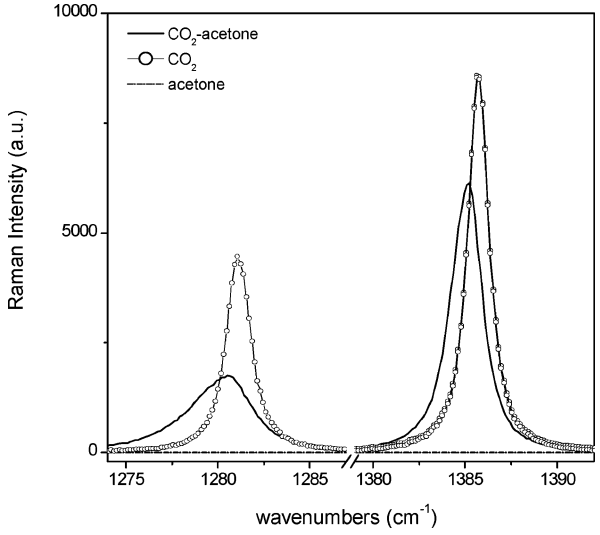

Figure 5. Polarized Raman spectra in the CO_2 Fermi dyad domain at 313 K of the CO_2−acetone mixture ($x_{CO_2} = 0.76$, $\rho = 829$ kg m^{-3}) (—) and of pure CO_2 (19 MPa, $\rho = 830$ kg m^{-3}) (—○—). The polarized spectrum of pure acetone under its vapor pressure is displayed for comparison (− · − · −).

4. $\nu_1-2\nu_2$ Fermi Dyad Spectral Domain

The interpretation of the pure CO_2 spectrum has been the subject of considerable work that has been thoroughly reviewed.[14] It is established that the $\nu_{\{2l\}}$ and $\nu_{\{2u\}}$ observed transitions originate from the resonance between the unperturbed energy levels associated with the fundamental transition ($\nu_1 = 0 \rightarrow 1$) of the ν_1 totally symmetric stretching mode and the harmonic transition ($\nu_2 = 0 \rightarrow 2$) of the ν_2 bending mode. The energy levels of the vibrational state $\nu_2 = 2$ are triply degenerated (2^0, $2^{\pm 2}$) with symmetry Σ^+_g and Δ_g, respectively.[15] The Fermi coupling only occurs between the ν_1 level with the 2^0 level which has the same symmetry (Σ^+_g) whereas the level Δ_g is unaffected by the Fermi resonance.[15,16]

4.1. Experimental Results. The Raman spectrum of the CO_2−acetone mixture for $x_{CO_2} = 0.76$ is compared with those of neat CO_2 and pure acetone in the Fermi domain in Figure 5 at similar density values. In this spectral range, the spectrum of pure acetone is flat, whereas the pure CO_2 spectrum exhibits two intense peaks. The CO_2 spectra in the mixture display the same features as those reported for neat CO_2. However, we observe that the band center position of the Fermi doublet is shifted toward lower frequency. In addition, the width of each of the two components, particularly the lower one, increases markedly compared to those of pure CO_2. The polarized Raman spectra of the CO_2 Fermi dyad measured in the binary mixtures at increasing carbon dioxide molar fraction are displayed in Figure 6. The intensities have been normalized to the total integrated intensity of each component of the dyad. They have been compared with the spectrum of pure CO_2 recorded at a density $\rho = 830$ kg m^{-3} which is close to the density of the more concentrated mixture ($\rho = 829$ kg m^{-3}). It is apparent that the marked spectral perturbations reported above become, as expected, less sizable as the concentration of CO_2 increases. However, it is noteworthy that a small amount of acetone added to CO_2 ($x_{CO_2} = 0.92$) leads to marked spectral perturbation (Figure 6).

The evolution with CO_2 concentration of the depolarization ratio $\rho = I_{HV}/I_{VV}$ of the {2u} and {2l} components are reported

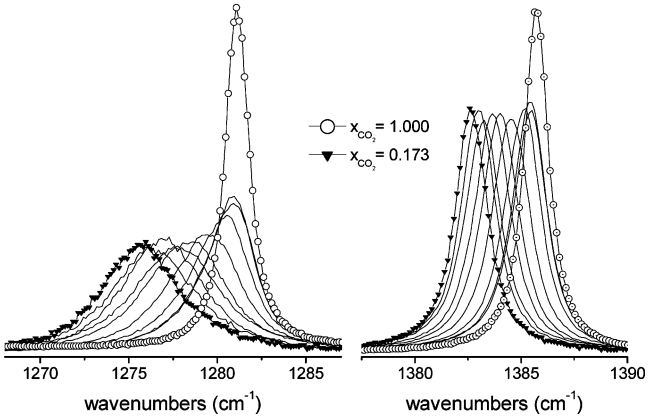

Figure 6. Evolution of the polarized Raman spectra of the CO_2 Fermi dyad at increasing CO_2 molar fraction in the binary mixtures at 313 K. The intensities have been normalized to the total integrated intensity of each component of the dyad. Spectra are displayed for the molar fractions 0.173 (—▼—); 0.300; 0.434; 0.495; 0.566; 0.664; 0.760; 0.833; 0.912; 1 (—○—) from left to right on each dyad component. The value of the density of pure CO_2 was chosen to be closed to those of the binary mixtures (ρ = 830 kg m^{-3}).

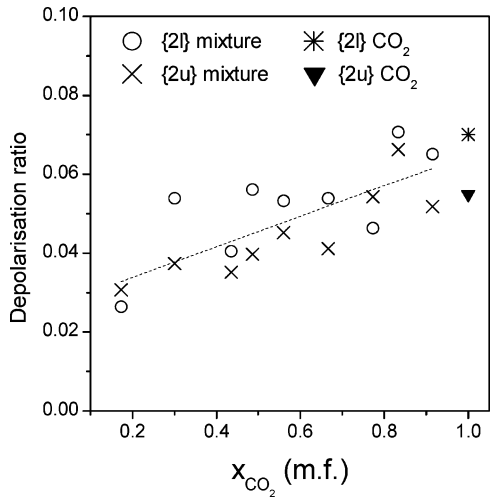

Figure 7. Evolution with the CO_2 concentration of the depolarization ratio $\rho = I_{HV}/I_{VV}$ of the {2u} (×) and {2l} (○) components of Raman spectra in the CO_2 Fermi dyad domain of CO_2−acetone mixtures at 313 K. The values for pure CO_2 (19 MPa, ρ = 830 kg m^{-3}) are displayed for comparison {2l} (*),{2u} (▼).

in Figure 7. In the density range investigated, the value of $\rho_{\{2u\}}$ and $\rho_{\{2l\}}$ are close to each other and increase linearly with the CO_2 concentration. As x_{CO_2} values get closer to unity, the values of $\rho_{\{2u\}}$ and $\rho_{\{2l\}}$ approach, as expected, the limiting values measured for neat CO_2 at the same temperature and density (Figure 7).

To get a more quantitative insight, the components have been analyzed by fitting the dyad band shapes with Lorentzian profiles. It is revealed that although fair fits are obtained, there still exist some discrepancies between the calculated and experimental band shapes (Figure 8a). It is only by fitting two Lorentzian profiles on each doublet components that very good fits have been achieved (Figure 8b). This finding confirms the results that we have reported for CO_2 neat SC fluid.[1,2]

We will denote the two fitted Lorentzian in the high-frequency component of the Fermi doublet as U_1 and U_2 (U standing for upper). The label 1 (resp 2) characterizes the fitted profile centered at the lowest frequency (resp higher). This convention will be also applied to the lowest component of the Fermi dyad denoted L_1, L_2 (L for lower).

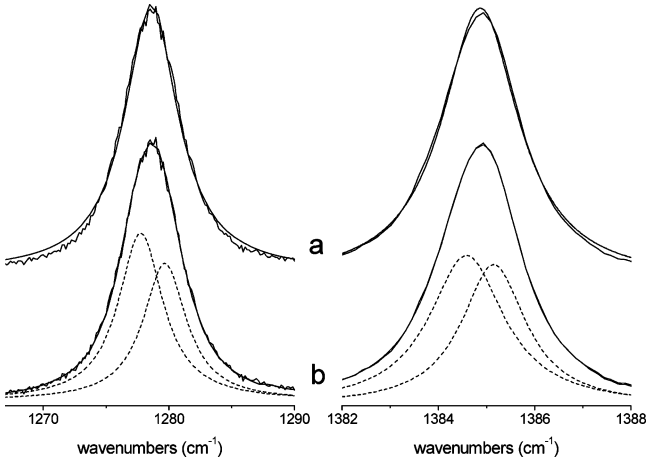

Figure 8. Experimental and calculated polarized Raman spectra in the CO_2 Fermi dyad domain of the CO_2−acetone mixture (x_{CO_2} = 0.434) at 313 K. The calculated band shapes have been obtained by fitting (a) one Lorentzian profile; (b) two Lorentzian profiles (on the left and on the right {2l} and {2u} components, respectively).

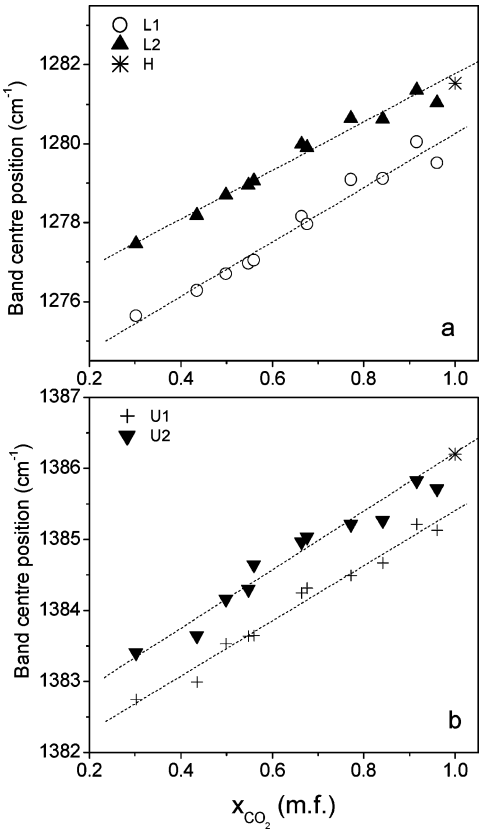

Figure 9. Evolution with the CO_2 concentration of the band center position of the fitted Lorentzian profiles to the polarized Raman spectra in the CO_2 Fermi dyad domain of CO_2−acetone mixtures at 313 K: (a) {2l} (○) L_1, (▲) L_2; (b) {2u} (+) U_1, (▼) U_2. The value for pure CO_2 (19 MPa, ρ = 830 kg m^{-3}) is displayed for comparison (*).

The evolution with the CO_2 concentration of the frequency positions and widths (FWHH) of the peaks L_1, L_2 and U_1, U_2 is displayed in Figures 9 and 10, respectively.

We found that the band center frequency values of the four fitted Lorentzian lines increase almost linearly with x_{CO_2} (Figure 9a,b). We note that the difference between the values of the band centers of either the U_1, U_2 profiles or the L_1, L_2 profiles are almost constant, but for the latter this difference is about double than for the former ones.

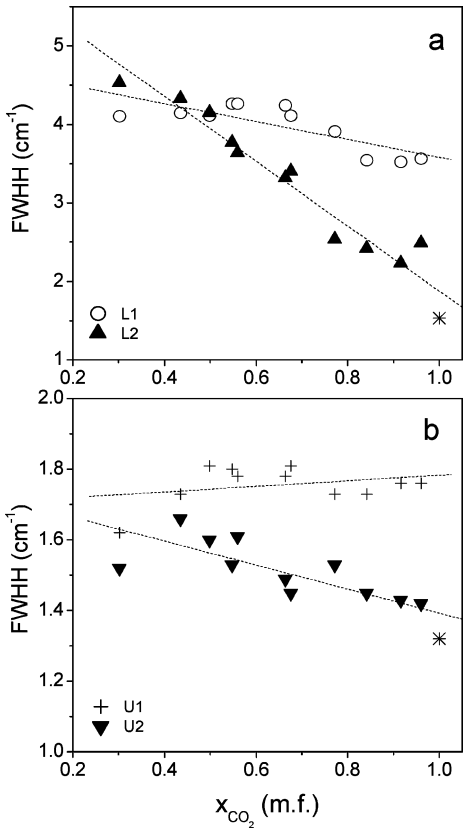

Figure 10. Evolution with the CO_2 concentration of the FWHH of the fitted Lorentzian profiles to the polarized Raman spectra in the CO_2 Fermi dyad domain of CO_2−acetone mixtures at 313 K: (a) {2l} (○) L_1, (▲) L_2; (b) {2u} (+) U_1, (▼) U_2. The value for pure CO_2 (19 MPa, $\rho = 830$ kg m^{-3}) is displayed for comparison (*).

The evolution of the width of all the profiles is almost linear with CO_2 concentration. Upon increasing the CO_2 content in the mixture, it is observed that the width of the L_2 profile decreases more strongly than that of the L_1 profile. In contrast, the widths of the U_1, U_2 which are narrower than L_1, L_2 are found to be less affected by the dilution effect.

The ratio $R = (I_{U1} + I_{U2})/(I_{L1} + I_{L2})$, where I denotes the integrated intensity of the Lorentzian lines, decreases continuously from about 2.5 at $x_{CO_2} = 0.17$ with increasing molar fraction of CO_2 and reaches an almost asymptotic value of about 1.75 at $x_{CO_2} = 0.92$ which is close to that measured for neat CO_2 at the same corresponding density (Figure 11a). We found that the values of the ratios $R_L = I_{L1}/I_{L2}$ and $R_U = I_{U1}/I_{U2}$ although presenting some dispersion, are the same within experimental uncertainties and decrease slightly with increasing concentration of CO_2 in the mixture (Figure 11b). Finally, we notice that the ratios $R_2 = I_{U2}/I_{L2}$ and $R_1 = I_{U1}/I_{L1}$ (Figure 11c,d) although presenting some dispersion lead to almost constant average values which are concentration independent.

4.2. Interpretation. The assignment of the four Lorentzian lines used to fit the experimental data can be rationalized by taking into account the existence of the transient acetone−CO_2 'complex'. In this framework, we expect to distinguish CO_2 molecules existing within two different type of environments. The first one is associated with CO_2 molecules specifically interacting with acetone molecules and likely engaged in the formation of a heterodimer. The second one corresponds to carbon dioxide mostly interacting with acetone but not in a specific way and that we will refer to in the following as the 'free' CO_2 molecules. In this framework, the Raman spectra should display four bands. Two of them should be associated with the Fermi dyad of the 'free' CO_2, whereas the two others should correspond to the dyad of CO_2 engaged in the complex. This is the situation that we have reported for neat SC CO_2 in which a homodimer was put in evidence.

We should emphasize that the so-called 'free' CO_2 molecules are different from that of pure CO_2 in the sense that the former molecules experience the dipolar field of acetone which clearly influence the spectral characteristic of the Fermi transition (see Figure 6 for example).

The next step is to assign the origin of each of the two profiles constituting the lower and the upper Fermi components to carbon dioxide in its two environments. We can perform this assignment by recalling that the values of the spectral characteristics of the two bands associated with the Fermi dyad of the 'free' CO_2 measured in the binary mixture should approach those measured in pure CO_2 in the limit of CO_2 molar fraction close to unity. Of course, in this comparison, the parameters of the Fermi dyad of the pure CO_2 should be taken from spectra measured at a density comparable to that of the binary mixture. To validate this statement and proceed with the proposed assignment, we have reported in Figure 9 the band center positions measured for the Fermi dyad of pure CO_2 at the density $\rho = 830$ kg m^{-3} ($P = 19$ MPa) which is very close to that of the more concentrated investigated mixture ($x_{CO_2} = 0.92$, $\rho = 829$ kg m^{-3}). It comes out that the evolution of the band center values of the L_2 and U_2 components with the CO_2 concentration in the mixture can be nicely extrapolated to the values measured for pure CO_2 (Figure 9). The same procedure has been applied to treat the evolution of the values of the width of the four components with the CO_2 concentration in the mixture. Again, it is found that the evolution of the widths of the L_2 and U_2 components can be nicely extrapolated to the values measured for pure CO_2 (Figure 10). Finally, we have performed the same method on the evolution of the ratio of the integrated intensity U_2/L_2 and U_1/L_1. It is revealed that the extrapolated value at $x_{CO_2} = 1$ of the former ratio compares favorably with the average value measured for pure CO_2 (Figure 11c,d).

Therefore, we may assign the U_2 and L_2 components to the signature of the Fermi dyad of 'free' CO_2, whereas the L_1 and U_1 components correspond to the CO_2 engaged in the heterodimer. It is noteworthy that this result is also consistent with that we have reported for SC CO_2, in which the corresponding L_1 and U_1 components have been assigned to the signature of the homodimer.

At this level, we may tentatively try to interpret these observations in the context of the theoretical treatment of the effect of chemical exchange on Raman band shapes.[17,18] In this framework, the chemical equilibrium can be considered as a dichotomic stochastic process between the so-called 'free' and complex sites of CO_2 according to

$$\underset{\text{'free'}}{CO_2} + \text{acetone} = \underset{\text{complex}}{CO_2\text{*acetone}} \qquad (4)$$

This theory involves τ_{obs} the Raman observation time and $\tau_{exchange}$ the chemical exchange time. The former is given by $\tau_{obs} = (c|\bar{\nu}_{bound} - \bar{\nu}_{free}|)^{-1}$ where $\bar{\nu}$ is the wavenumber value of the band center position corresponding to the transitions of the 'bound' and 'free' CO_2 within each component of the dyad. The latter is defined from the association and dissociation rate constant of CO_2 between its two sites as $\tau_{exchange} = (k_a[\text{acetone}] + k_d)^{-1}$.

Two limits are considered. In the slow exchange limit, $\tau_{obs} < \tau_{exchange}$, the bands of the free and bound species can be

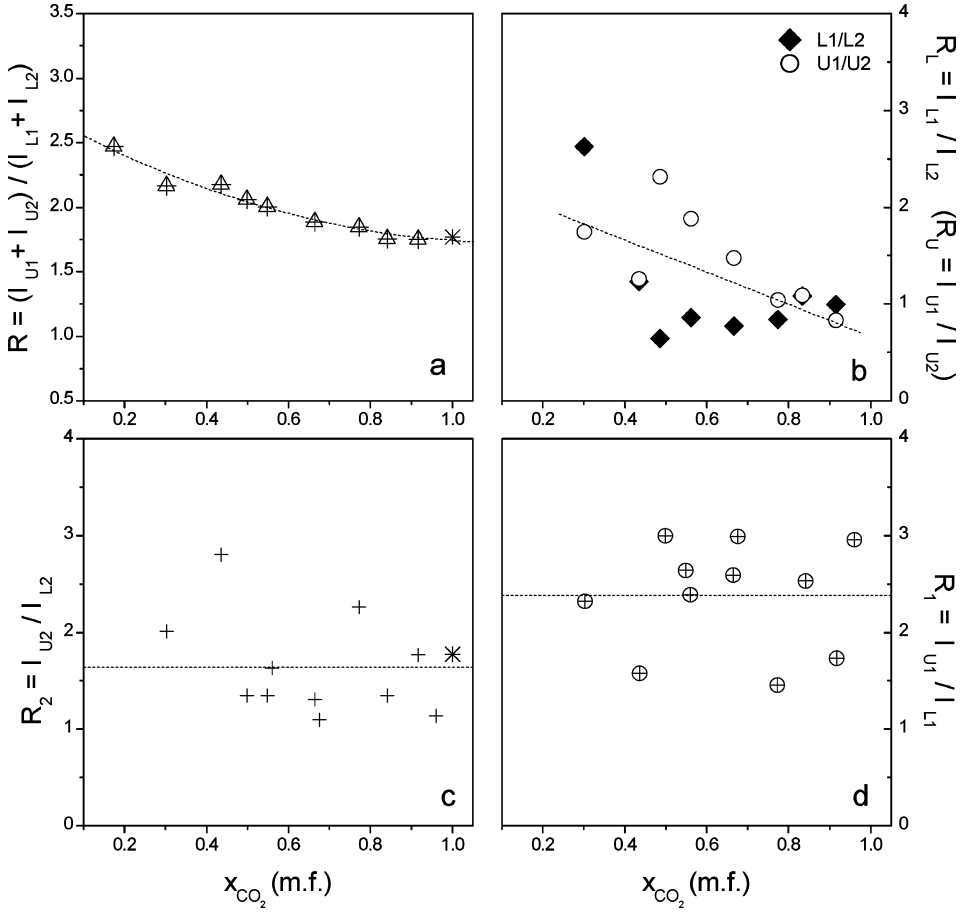

Figure 11. Evolution with the CO_2 concentration of the ratio of integrated intensities I of the polarized profiles in the CO_2 Fermi dyad domain at 313 K of CO_2−acetone mixtures: (a) $R = (I_{U1} + I_{U2})/(I_{L1} + I_{L2})$; (b) $R_L = I_{L1}/I_{L2}$ (◆) and $R_U = I_{U1}/I_{U2}$ (○). The corresponding R values for pure CO_2 (19 MPa, $\rho = 830$ kg m^{-3}) are displayed for comparison (*).

detected, and four bands should be observed on the Fermi dyad. In contrast, if $\tau_{obs} > \tau_{exchange}$ the fast exchange limit is recovered, and the doublet structure of each component of the Fermi dyad should collapse. Between these extreme situations, the doublets are not completely resolved, and a band-shape analysis of the mixture obtained in a broad concentration range should allow a discussion of the contribution of the exchange dynamic on the profiles broadening.[19] Actually, this latter situation is that encountered in our experiments. However, to the best of our knowledge, a quantitative treatment cannot be performed as the theory of chemical exchange of Raman modes undergoing Fermi resonance is not available. It should be also stressed that even for nonresonant mode, the application of such theory requires a large number of parameters which are unknown here and would certainly hamper a quantitative treatment. Therefore, we will discuss our results only on the grounds of physical arguments. The Raman observation times τ_{obs} estimated from the band center frequency corresponding to the transitions of the 'bound' and 'free' CO_2 molecule of the upper and lower Fermi transition are 4 and 8 ps, respectively. Clearly, we can infer that the life time of the complex is in the picosecond range. This is consistent with the information extracted from the $\nu_2^{(1)}$ band. The width of this band leads to a typical time of about 500 fs for the relaxation processes. Clearly, during the life time of the complex, these processes can relax and condition the $\nu_2^{(1)}$ band shape.

A last step can be undertaken in estimating X, the population of the heterodimer versus the monomer, according to the reaction scheme (eq 4) and using the intensities of the L2 and L1 transitions. These intensities are respectively given by

$$I_{L1} = I_{Dimer} = A\alpha^2_D \text{ [dimer]}$$

$$I_{L2} = I_{Mono} = A\alpha^2_M \text{ [monomer]} \quad (5)$$

in which A is a geometric factor depending upon the scattering geometry, α^2 is the transition polarizability derivative associated with the dimer or the monomer spectral transition, and the brackets denote the molecular concentration of the two species. We are led to a value for X given by $X = (I_{L1}/I_{L2})/(\alpha^2_D/\alpha^2_M)$. Because Raman cross-sections are unknown, we suppose that they are unaffected by molecular aggregation. Indeed, it was established that even when strong specific interactions between molecules are involved, as for instance in hydrogen-bonded clusters of alcohols,[20] such a molecular quantity is not strongly affected by the state of aggregation. In addition, ab initio calculations performed in the frame of the harmonic hypothesis (absence of Fermi resonance) show that the activity of the ν_1 mode is almost the same for the isolated CO_2 molecule and for the CO_2 engaged heterodimer.[21] Within this hypothesis, the values of the ratio I_{L1}/I_{L2} lead to X decreasing from 2 to 0.8 with the CO_2 concentration. As expected, the same conclusions apply for the upper transitions. This means that the proportion of CO_2 engaged in the heterodimers decreases from about 70% to 40% with CO_2 concentration.

5. Spectral Domain Between the Dyad Peaks

5.1. Experimental Results. We found in the spectra of the mixture the presence of a very weak feature (absent in pure

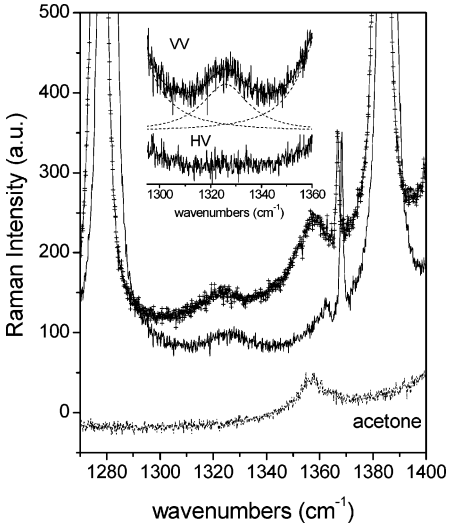

Figure 12. Polarized Raman spectra in the spectral domain between the CO_2 Fermi dyad peaks in CO_2−acetone mixtures at 313 K: (−) $x_{CO_2} = 0.912$ and (−+−) $x_{CO_2} = 0.434$; the polarized spectrum of pure acetone under their vapor pressure is presented for comparison. I_{VV} and I_{HV} profiles for $x_{CO_2} = 0.912$ CO_2−acetone mixture are displayed in the inset at the top.

acetone) centered at about 1320 cm^{-1} which is polarized ($\rho =$ 0.35 at 7.35 MPa). The corresponding spectra are presented for two concentrations of CO_2 in the mixture (Figure 12). From profile decomposition in this domain, we found that the band shape is Lorentzian with a full width of 16 ± 1 cm^{-1}

5.2. Interpretation. In order to interpret the origin of this new feature, we remembered that for the isolated CO_2 molecule the $0 \rightarrow \Delta_g$ transition should be observed in this spectral domain with a Raman cross-section 2 orders of magnitude lower than those of the doublet.[16] We could assign the feature detected in the mixture to this transition. However, it is predicted that the transition should be depolarized in a marked contrast with the observations. The activity and polarization of the experimental transition can be rationalized in the framework of a complex formation between CO_2 and acetone molecules. Indeed, due to this intermolecular interaction, the double degeneracy of the Δ_g level should be removed, and hence two transitions should be observed. The symmetry and polarization of these two modes can be predicted using the correlation method between the $D_{\infty h}$ point group of the free CO_2 molecule and the point group of the dimer. On the basis of the fact that the more energetically favored complex should be of C_s symmetry according to ab initio calculations,[3] A′ (polarized) and A″ (depolarized) transitions should be observed. We surmise that the observed feature can be assigned to the polarized A′ transition and that the activity of A″ is negligible compared with the former transition. It noteworthy that the previous feature has also been observed in pure SC CO_2 at about 1332 cm^{-1} [11] and has contributed to support the existence of the homodimer formation in the fluid.

6. Discussion

The concept of complex can been rationalized on the grounds of investigations performed previously on weak complexes putting emphasis on the nature and time scale of the interactions in connection with the spectroscopic time window of observation. Random orientations of the acetone and CO_2 molecules in the mixture exist and it is for a particular structural arrangement that the specific interaction (EDA) between acetone and CO_2 molecule can act to lead to a 'transient complex' during the time scale of the experimental observation.[22] CO_2 molecules not involved in this particular arrangement still interact with acetone but not specifically leading to the so-called 'free' CO_2. This picture has been developed a long time ago by Mulliken and co-workers[23] in their investigations of contact charge transfer (CT) complexes using thermodynamic considerations involving multiple chemical equilibria. A first equilibrium exists between the electron donor−acceptor moieties leading to the formation of a 1:1 complex, and a second equilibrium is established between the electron acceptor center and the solvent.[24] The latter equilibrium is the counterpart of what we call here the 'free' CO_2. However, the difficulty encountered at that time in trying to rationalize spectroscopic data (mostly UV−visible spectroscopy) in terms of thermodynamics still exists in our investigation. One of the main concerns was related to the very low values of the equilibrium constant ($K_C < 0.01$ l mol^{-1}) of contact CT complexes reported experimentally. The significance of such low values was questioned from the thermodynamic point of view. The objection was grounded on collision theory which shows that random encounters of molecules in a thermal bath lead to a value of the equilibrium constant close to 0.30 l mol^{-1} at room temperature.[22,25] We are faced here with the same situation in view of the value of the equilibrium constant that we obtained from the $\nu_2^{(1)}$ band analysis. Incidently, it is noteworthy to remember that the equilibrium constants of CO_2 Lewis bases systems diluted in an "inert" solvent (*n*-pentane) have been measured by FTIR spectroscopy.[4] In particular for the system CO_2−triethylamine (TEA) in which TEA is a slightly stronger base than acetone,[12] a value of K_C of about 0.046 mol L^{-1} has been reported. This value, although 1 order of magnitude greater than ours, is still below the predicted one by collision theories. However, it was subsequently shown that K_{obs} the "observed" equilibrium constant, results from the difference between the true equilibrium constant K_C and that associated with random collisions (K_{random}). Finally, it was demonstrated that the observed equilibrium constant K_{obs}, named after Guggenheim[26] 'sociation' equilibrium constant, is physically significant when a theoretical model is available for calculating K_{random}.

The second issue raised concerns regarding the consistency between the values of the equilibrium concentration *C* of the heterodimer versus the total concentration of CO_2 deduced from the analysis of the $\nu_2^{(1)}$ band and from the Fermi dyad. In the former case, the *C* value is about 1% whereas it is comprises between 70 and 40% in the latter case. Clearly, these features do not agree. Assuming that the true equilibrium concentration *C* is provided from the direct analysis of the $\nu_2^{(1)}$ band, it is possible to obtain a consistent result by arguing that the Raman cross sections corresponding to the Fermi dyad of the heterodimer are very different than that of the monomer. As a matter of fact, the Raman cross sections corresponding to the heterodimer should be about 30 times greater than that corresponding to the monomer. In the absence of theoretical studies, this is an open question and it is hard to conclude. At this level, let us remember that the values of the equilibrium concentration *C* for the heterodimer in the acetone−CO_2 mixture are comparable with that obtained for the homodimers in neat CO_2 for which C is about 40%.[1] The latter value was found to be consistent with the results reported from others investigations.[27] It should be pointed out that in all the investigations, including the current one, the Raman cross sections of CO_2 are supposed nearly unaffected by the complex formation phenomenon.[1]

We come to the conclusion that the equilibrium constant reported here should be only considered for discussion in the absence of a theoretical model for calculating K_{random}.[22] We also

emphasize that the method to get equilibrium concentration through the Fermi dyad needs to be more firmly theoretically grounded. In this context, the treatment of Raman spectra of transitions involving a Fermi resonance when species probe different environments, as here, need to be considered to assess the validity of the population concentration experimentally obtained.

7. Conclusion

One of the main issues coming out from this study concerns the interpretation of the intermolecular interactions between CO_2 and acetone as the signature of the charge-transfer complex predicted by ab initio calculations. Clearly, this viewpoint is supported directly by the observation of the $\nu_2^{(1)}$ band of CO_2. Moreover, the analysis of the Fermi dyad and the feature detected in the domain extending between the former doublets have reinforced this viewpoint and also lead us to the conclusion that CO_2 should exist in two different environments. However, the equilibrium concentrations of the complex obtained from the $\nu_2^{(1)}$ spectral domain and from the Fermi dyad domain appear to be different. This situation is probably due to the absence of a theoretical approach of Fermi resonance transitions associated to species existing in different environments.

Acknowledgment. The University of Bordeaux 1 and the Fundação para a Ciência e Tecnologia (Portugal) are acknowledged for the financial support of M.I.C. The joint CNRS-GRICES PICS program no. 3090 has provided travel and stay facilities for M.I.C. and M.B. to complete part of this work. Authors are pleased to thank David Talaga and Jean-Luc Bruneel of the ISM for valuable help in Raman measurements.

References and Notes

(1) Cabaço, M. I.; Longelin, S.; Danten, Y.; Besnard, M. Submitted, 2007.

(2) Cabaço, M. I.; Longelin, S.; Danten, Y.; Besnard, M. Accepted *J. Phys. Chem. A*, 2007.

(3) Danten, Y.; Tassaing, T.; Besnard, M. *J. Phys. Chem. A* **2002**, *106*, 11831.

(4) Meredith, J. C.; Johnston, K. P.; Seminario, J. M.; Kazarian, S.; Eckert, C. A. *J. Phys. Chem. A* **1996**, *100*, 10387.

(5) Dobrowolski, J. C.; Jamroz, M. H. *J. Mol. Struct.* **1992**, *275*, 211.

(6) Cabaço, M. I.; Danten, Y.; Tassaing, T.; Longelin, S.; Besnard, M. *Chem. Phys. Lett.* **2005**, *413*, 258−262.

(7) Chang, C. J.; Day, C.-Y.; Ko, C.-M.; Chiu, K.-L. *Fluid Phase Equilib.* **1997**, *131*, 243.

(8) Bowman, L. E.; Palmer, B. J.; Garett, B. C.; Fulton, J. L.; Yonker, C. R.; Pfund, D. M.; Wallen, S. L. *J. Phys. Chem.* **1996**, *100*, 18327.

(9) Danten, Y.; Tassaing, T.; Besnard, M. *J. Mol. Liq.* **2005**, *117*, 49.

(10) Danten, Y.; Tassaing, T.; Besnard, M. *J. Chem. Phys.* **2005**, *123*, 074505.

(11) Lalanne, P.; Rey, S.; Cansell, F.; Tassaing, T.; Besnard, M. *J. Supercrit. Fluids* **2001**, *19*, 199.

(12) Jamroz, M. H.; Dobrowolski, J. C.; Bajdor, K.; Borowiak, M. A. *J. Mol. Struct.* **1995**, *349*, 9.

(13) Ford, T. A. Ab Initio Predictions of the Vibrational Spectra of Some Molecular Complexes: Comparison with Experiment. In *Molecular Interactions*; Schneider, S., Ed.; John Wiley & Sons Ltd.: New York, 1997; pp 181.

(14) Garrabos, Y.; Echargui, M. A.; Marsault-Herail, F. *J. Chem. Phys.* **1989**, *91*, 5869 and references therein.

(15) Herzberg, G. In *Molecular Spectra and Molecular Structure: Infrared and Raman Spectra of Polyatomic Molecules*; D. Van Nostrand Company, Inc.: Princeton, NJ. 1956; Vol. II, pp 217.

(16) Montero, S. *J. Chem. Phys.* **1983**, *79*, 4091.

(17) McPhail, R. A.; Strauss, H. L. *J. Chem. Phys.* **1985**, *82*, 1156.

(18) Bratos, S.; Tarjus, G.; Viot, P. *J. Chem. Phys.* **1986**, *85*, 803.

(19) Besnard, M. Chemical Kinetics and Vibrational Spectroscopy: an analysis of weak charge-transfer complexing reactions. In *Molecular Liquids: New Perspectives in Physics and Chemistry*; Teixeira-Dias, J. J. C., Ed.; Kluwer Academic Publishers: Dordrecht, 1992; pp 469.

(20) Lalanne, P.; Andanson, J. M.; Soetens, J.-C.; Tassaing, T.; Danten, Y.; Besnard, M. *J. Phys. Chem. A* **2004**, *108*, 3902.

(21) Danten, Y. 2007, private communication.

(22) Scott, R. L. *J. Phys. Chem.* **1971**, *75*, 3843.

(23) Mulliken, R. S. *J. Am. Chem. Soc.* **1952**, *74*, 811.

(24) Orgel, L. E.; Mulliken, R. S. *J. Am. Chem. Soc.* **1957**, *79*, 4839.

(25) Prue, J. E. *J. Chem. Soc.* **1965**, 7534.

(26) Guggenheim, E. A. *Trans. Faraday Soc.* **1960**, *56*, 1159.

(27) Huisken, F.; Ramonat, L.; Santos, J.; Smirnov, V. V.; Stelmakh, O. M.; Vigasin, A. A. *J. Mol. Struct.* **1997**, *47*, 410−411.